Catalysis Today 138 (2008) 77–83

Contents lists available at ScienceDirect

Catalysis Today

journal homepage: www.elsevier.com/locate/cattod

Theoretical study of methane adsorption on perfect and defective Ni(1 1 1) surfaces

M.F. Haroun [a], P.S. Moussounda [a,b], P. Légaré [a,*]

[a] Laboratoire des Matériaux, Surfaces et Procédés pour la Catalyse (LMSPC), UMR 7515, CNRS-ECPM, Université Louis Pasteur, 25 rue Becquerel, 67087, Strasbourg Cedex 2, France

[b] Groupe de Simulations Numériques en Magnétisme et Catalyse, Département de Physique, Faculté des Sciences, Université Marien NGouabi, BP 69 Brazzaville, Congo

ARTICLE INFO

Article history:
Available online 13 June 2008

Keywords:
Methane adsorption
Perfect and defective Ni(1 1 1) surfaces
Ni adatom

ABSTRACT

We employ periodic density functional theory (DFT-GGA-PW91) calculations to study the adsorption of CH_4, on a perfect and defective (1 1 1) face of nickel, at a coverage of 0.25 monolayer (ML). As a surface defect, we consider a Ni adatom. We investigate systematically the site preference for CH_4, for various molecular orientations with 1, 2 or 3 H pointing toward the surface. Whatever the CH_4 adsorption site could be, the most stable configurations are obtained when 2 H atoms are directed to the surface. CH_4 stabilises weakly on the flat Ni surface, the adsorption energies being at best in the 50 meV range. However, beside a dominating physical interaction, some features are indicative of a chemical interaction through the Ni d-band. In presence of a Ni adatom, the chemical nature of the interaction manifests plainly, with sizeable adsorption energies up to 0.37 eV. The molecular restructuring and the mechanism of the interaction are examined.

1. Introduction

The interaction of CH_4 with transition metal (TM) surfaces has been explored extensively in these last years by many experimental surface techniques [1–5] and theoretical investigations [6–10]. As CH_4 is the simplest of all alkanes, its dissociation can be viewed as prototypical for C–H activation in catalysis. Nevertheless its dominant mechanisms on transition metal surfaces remains the subject of controversy, despite the numerous investigations on the subject [11–13]. Indeed, methane chemisorption has been studied on TM by employing both molecular beam experiments as well as "bulb" techniques. Temperature programmed desorption (TPD) experiments showed that the interaction of methane with TM surfaces is weak [4]. On Pt(1 1 1) it desorbs at 67 K. However, when trapped on terraces, it can migrate to steps from which the desorption temperature is 140 K [14]. This shows that low-coordinated atoms may play a substantial role for methane adsorption and activation. It has also been shown that dissociation of methane on TM proceeds via either a direct dissociative mechanism [15–17] or a precursor/trapping mediated mechanism [18,19]. Both mechanisms are surface structure sensitive but the latter is likely to be especially influenced by surface defects. On low index faces of Ni, the direct mechanism seems to be dominating [13,20]. This is in line with the low interaction of the CH_4 molecule on these surfaces. This also suggests that it could be different on low-coordinated sites.

In this paper, our aim is to illustrate how a low-coordinated adsorption site, namely a Ni adatom, could modify the interaction of CH_4 with a Ni(1 1 1) surface. This adatom and the perfect (1 1 1) surface represent respectively the lowest and the highest Ni surface coordination, corresponding to two opposite cases in the expected degree of molecular interaction with a solid surface. They are also a first step toward a future comparison of the possible CH_4 dissociative pathways. Moreover, the reactivity of an adatom was rarely examined [21,22], and never on Ni. We outline that focusing on the adatom behaviour could be considered as an approach toward situations encountered on catalysts metallic aggregates where low-coordination surface atoms are likely to play a crucial role.

2. Theoretical method

All simulations in this study were conducted using the Danish *ab initio* pseudopotential code Dacapo [23]. This program is based on density functional theory (DFT). The Kohn-Sham one electron valence states are expanded on a plane waves basis set, and ionic

* Corresponding author.
E-mail address: legare@chimie.u-strasbg.fr (P. Légaré).

0920-5861/$ – see front matter © 2008 Elsevier B.V. All rights reserved.
doi:10.1016/j.cattod.2008.04.040

cores are described by ultrasoft pseudopotentials [24]. In our calculations, the exchange-correlation potential and energy are described self-consistently using the generalised gradient approximation of the Perdew-Wang functional (GGA-PW91) [25]. The plane wave basis set was limited by a 400 eV energy cutoff. The surface irreducible Brillouin zone was sampled by 13 special k-points using a $(5 \times 5 \times 1)$ Monkhorst-Pack grid. A Fermi broadening corresponding to $k_BT = 0.1$ eV was employed to help convergence (k_B is the Boltzmann constant). Total energies are then extrapolated to $T = 0$ K. As spin-polarized computation is a quite demanding task, we used non-spin-polarised calculations only. Limited spin-polarised calculations indicate that the overall behaviour reported below is conserved.

For the results presented here, a slab formed by four layers of Ni(1 1 1) was used with a (2×2) surface unit mesh. The adsorbed species was located on one face only of the slab, thus giving a coverage of 0.25 monolayer (ML). The adsorbate and the Ni plane underneath were allowed to relax freely, the other Ni planes being frozen in the Ni bulk configuration. The slab is reproduced periodically in the perpendicular direction, the images being separated by a vacuum region equivalent to five interlayer Ni(1 1 1) spaces, or ~10 Å thick. The calculated equilibrium lattice constant for bulk Ni is 3.525 Å, in close agreement with the experimentally determined value of 3.524 Å[26] and with other theoretical evaluation using similar methods [27]. The sum of all forces were converged below 0.05 eV/Å. For calculations involving a Ni adatom, the latter was located in hollow fcc site which was 0.03 eV more stable than the hollow hcp site. The adsorption energies E_{ads} are calculated following

$$-E_{ads} = E_{adsorbate/Ni} - E_{Ni} - E_{adsorbate}$$

where $E_{adsorbate/Ni}$ represents the total energy of the Ni(1 1 1) slab after adsorption, E_{Ni} the total energy of the clean relaxed Ni(1 1 1) slab and $E_{adsorbate}$ that of the free adsorbate in the gas phase provided by the DFT calculations. The minus sign at the left-hand side ensure that E_{ads} is positive for a stabilising adsorption.

The electronic structure was analysed with use of the projected density of states (PDOS) on an atomic basis limited to a spherical space around the atoms of interest, with a radius of 0.85 Å for the constituents of the molecule and 1 Å for Ni.

3. Results and discussion

As our aim is to compare the interaction of CH_4 with the Ni(1 1 1) surface and with a Ni adatom deposited on the same surface, we report on Fig. 1 the 3d density of state projected on a Ni atom of the perfect surface and on the Ni adatom. The narrowing of the latter with respect to the former is the obvious consequence of the low-coordination number of the adatom. Moreover, its valence d-band exhibit a high density around −0.4 eV which is not present on the flat surface. Hence, we expect that these two electronic systems exhibit a high difference in their interaction with a molecule.

3.1. CH_4 adsorption on perfect Ni(1 1 1) surface

Initially, we checked that the properties of the isolated CH_4 were accurately reproduced. The calculated gas phase C–H bond length and H–C–H angle were 1.097 Å and 109.5°, respectively in good agreement with experimental values [26]. The Ni(1 1 1) surface exhibits four high-symmetry adsorption sites as shown in Fig. 2. The adsorbed species could be located on top, bridge, fcc hollow or hcp hollow sites, hereafter labelled t, b, f and h, respectively. Several orientations of CH_4 were examined at each site. We designated the resulting configuration by the label of the

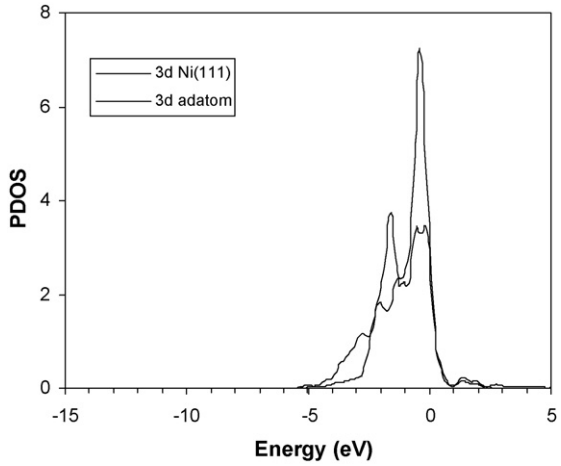

Fig. 1. d projected density of states for a clean Ni atom of the (1 1 1) surface (dashed line) and a Ni adatom (full line). The Fermi level is the origin of the energy scale.

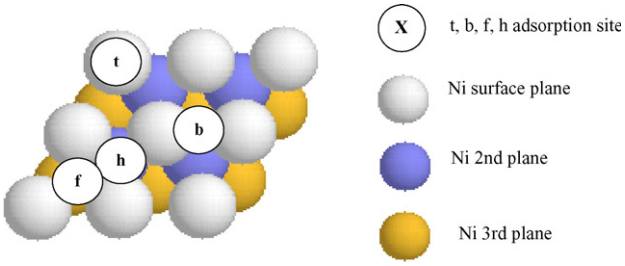

Fig. 2. Top view of the (2×2) Ni(1 1 1) perfect surface with the t (top site), b (bridge site), f (fcc hollow site) and h (hcp hollow site).

adsorption site plus the number (1–3) of H atoms pointing toward the surface before geometrical optimisation. In the case of the bridge site, we considered only the b1 and b2 configurations. In the case of b2 configuration, two different orientations of CH_4 were considered. The axis crossing the 2 H directed to the surface could be aligned or perpendicular with respect to the Ni–Ni bond. These two orientations were designated by b2a and b2p, respectively. Fig. 3 shows the orientations of methane on perfect Ni(1 1 1) surface at different sites after optimisation. We note that the symmetry of the starting configuration is generally conserved except for b2p and f2. Calculated adsorption energies and structural parameters for molecular configurations on the various sites are listed in Table 1. Clearly, we see that these adsorption energies are very small ranging from 34 meV to 53 meV. As it is known that DFT does not properly treat these weak interactions we cannot seriously discriminate between each of these values. For our purpose however, the most important is that we can take these results as references for the following study concerning the effect of a Ni adatom. This weak interaction of methane on late transition metals has been observed previously by Au et al. [28] in their DFT cluster calculations and by Yang and Whitten [29] in a study of adsorption of CH_4/Ni(1 1 1) with their ab initio CI cluster model. This is also in agreement with more recent works by Lai et al. [30] on Ni(1 0 0), Moussounda et al. [31] on Pt(1 0 0) and Sorescu [32] on Fe(1 0 0) using DFT periodic slab calculations.

For all configurations, the longest C–H bond length indicated in Table 1 always correspond to the H atoms pointing toward the surface. However, they do not differ appreciably from those of the gas phase molecule except when one H only is directed to the surface. Note that the C–Ni distance is longer when 2 H are directed to the surface in all the adsorption sites, specially for h2 adsorption. In fact, the height over the surface does not depend on the

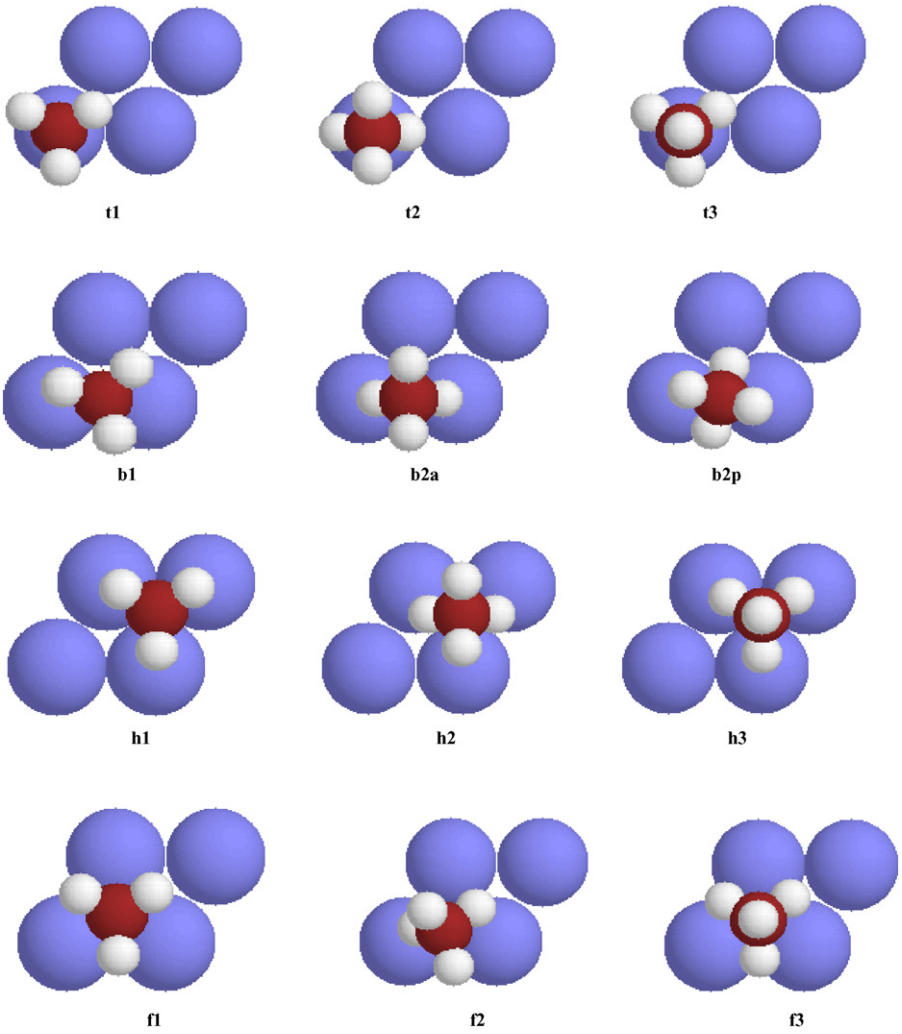

Fig. 3. Top view of the t, b, h and f configurations of CH_4 adsorbed on Ni(1 1 1) after geometrical optimisation.

Table 1
Calculated adsorption energies and structural parameters for CH_4 adsorbed at the four high-symmetry sites of the perfect Ni(1 1 1) surface. Several possible orientations of CH_4 at each site of Ni(1 1 1) are considered

Adsorption sites	Adsorption energy (meV)	Longest C–H bond length (Å)	C–Ni distance (Å)	Largest H–C–H angle (°)	Smallest H–C–H angle (°)
t1	35	1.104	3.463	110.1	108.8
t2	53	1.098	3.829	109.8	109.2
t3	34	1.098	3.487	109.7	109.3
b1	46	1.101	3.779	109.9	109.0
b2a	52	1.098	4.033	109.8	109.1
b2p	51	1.098	4.032	109.8	109.2
f1	39	1.102	3.865	109.9	109.1
f2	52	1.099	3.993	109.7	109.2
f3	34	1.098	3.761	109.7	109.2
h1	41	1.102	3.853	109.9	109.0
h2	52	1.098	4.092	109.8	109.2
h3	34	1.098	3.758	109.7	109.2

adsorption site, but essentially on the number of binding H. The observation of the H–C–H angles shows that they decrease when at least one of the hydrogen atoms points to the surface. On the contrary, they expand when the H atoms are directed to the vacuum region. This has also been observed on Pt(1 0 0) [31].

We turn now our attention to the electronic properties of the adsorbed species. In Fig. 4 we have plotted the sum of the s and p projected electronic states (PDOS) of the adsorbed molecule in the t1 configuration. We outline that the picture for the other configurations would not be much different. The curve exhibits two peaks centred at −12.2 eV (α) and −4.7 eV (β). They correspond respectively to H(s) + C(s) and H(s) + C(sp) states. Actually, these peaks are quite similar to those of the free molecule, which positions are indicated by vertical arrows in Fig. 4 after fitting of the vacuum levels of the covered surface with that of the free molecule. Clearly, the peaks are essentially shifted by 0.8 eV and 0.9 eV, respectively to the higher binding energies when CH_4 is adsorbed on the surface. This correlates with a Ni work-function

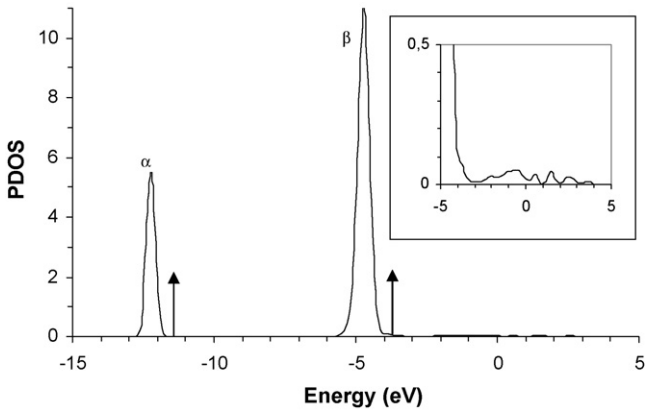

Fig. 4. Projected density of states of the CH_4 molecule adsorbed in the t1 configuration on the perfect Ni(1 1 1) surface. A zoom on the Fermi level region in given as inset. The position of the free molecule levels with respect to the covered Ni vacuum level is indicated by vertical arrows. The Fermi level is the origin of the energy scale.

decrease $\Delta\Phi$ = −0.40 eV indicating some polarisation induced by the molecule/surface contact as already reported for organic molecules adsorbed on metal surfaces [33]. However, we note that the shift suffered by the CH_4 electronic states is not uniform. Moreover, some broadening is apparent for the adsorbed molecule, specially on the −4.7 eV peak. Finally, as visible in Fig. 4 inset, some dispersed weak states appear from −4 eV up to 4 eV. They are essentially C sp states. Hydrogen s states contribute also in this region, mainly from the H atom directed to the Ni surface. This indicates that a faint mixture with Ni states takes place. We note that the induced electronic states are only partially occupied suggesting that they are of attractive character. The electron counting on the various atoms of the molecule and of the Ni surface is almost unchanged after adsorption. Clearly, surface-molecule charge transfer is not responsible of the above-mentioned polarisation. This means that the strong surface dipole revealed by the work-function decrease is the result of internal polarisations of the molecule on one hand, of the surface on the other hand, due to their mutual interaction and the electron redistribution described above. In order to clarify the interactions taking place between CH_4 and the Ni surface, we examined the sp (not shown) and d (Fig. 5) PDOS changes resulting from CH_4 adsorption for the

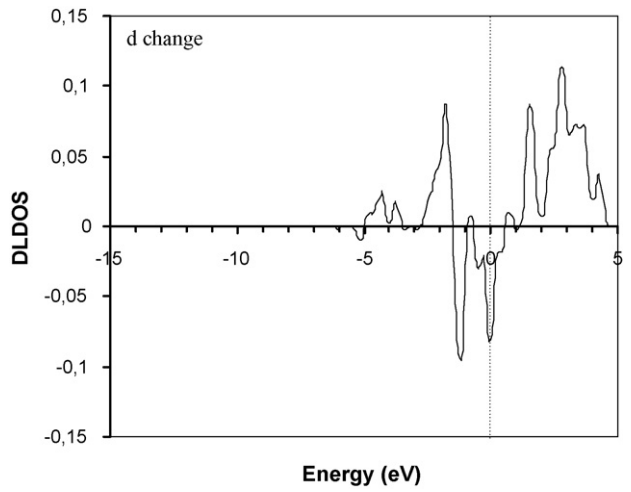

Fig. 5. Ni d projected density of states change upon CH_4 adsorption on the perfect Ni(1 1 1) surface with a t1 configuration. The Fermi level is the origin of the energy scale.

Ni atom located below the molecule. Changes induced on sp electrons are very weak and the d changes reported on Fig. 5 are about ten times more intense. So the Ni sp states are of secondary importance in the interaction with the molecule. Electronic d states are gained from −5 eV up to −2 eV, principally dz^2 around −4.5 eV and −3.8 eV, and mostly d*xz* and d*yz* around −1.75 eV. These states are lost around −1 eV and in the Fermi level (FL) region. Unoccupied states are gained around 1.5 eV, mostly dz^2, d*xz* and d*yz*. Moreover, we find a strong d gain from 2 eV up to 4 eV, a region where d states were totally absent on the clean surface. Hence the states detected on the molecule from −2 eV up to the FL are clearly the result of CH_4 interaction with the out-of-plane d states of Ni. The overall picture is that states disappear around the Fermi level resulting in a depressed region separating gains in stabilised occupied states below −1.5 eV and destabilised unoccupied states above 2 eV. These observations can be rationalised considering several weak orbital interactions. First, coupling between occupied CH_4 states and occupied Ni d states (O–O interaction) contribute to bonding d states around −4 eV and antibonding d states around −2 eV giving an overall nonbonding or slightly repulsive (Pauli) interaction. Owing to the molecule–surface distance, this interaction is very limited. Then we have to consider the two occupied-unoccupied (O–U) interactions between CH_4 and Ni. Note that, as unoccupied orbitals are more spatially extended than occupied orbitals, these are more likely to be effective than O–O interaction. We consider O(CH_4)–U(Ni) interaction first. This would give bonding states below the Fermi level, whereas antibonding states would locate above FL. Considering the Ni d states change (Fig. 5), the former could be around −4 eV and the latter around +2 eV or above, accounting for the lost of d states around FL. This provides a net bonding effect. Similarly, the O(Ni)–U(CH_4) would result in supplementary bonding effect, depopulating the upper occupied d-band region and accounting for the d gain around −2 eV whereas antibonding states would be pushed above +2 eV. These two interactions would lead to charge transfer from the molecule to Ni for the O(CH_4)–U(Ni) interaction, and to a back-donation from Ni to the molecule for the O(Ni)–U(CH_4) interaction. The net resulting charge transfer effect we can expect would be very limited as confirmed by electron counting, but this would also promote some electron redistribution. Indeed, we found that CH_4 adsorption induces dz^2 loss and d*xz*–d*yz* gain on the interacting Ni atom, s loss on the closest H atom to the surface, p*z* loss and s gain for C.

Finally the overall picture is that, beside an essentially physical interaction manifested by a shift of electrostatic origin, a weak donation and back-donation electronic exchange is apparent. It has already been showed that despite the well-known deficiency of our GGA method to describe the physical interaction between hydrocarbons and transition metal surfaces, the strong work-function change induced by the molecule can be accounted for [33] and that some chemical interaction indeed takes place [34].

3.2. CH_4 adsorption on the Ni adatom

Several configurations of the CH_4 molecule adsorbed close to the Ni adatom were examined. Here we present only results obtained with the molecule adsorbed on top of the adatom, designated by t1, t2 and t3 with similar meanings than above. Actually these configurations are not perfectly symmetric as could be suggested by the above nomenclature. They are however representative of configurations resulting from a dominating attractive force centered on the adatom. Other less symmetric configurations, tilted to the adatome nearest neighbours were also examined but they did not reveal energetically more interesting than the worst of the cases presented in Table 2. Examination of the

Table 2
Calculated adsorption energies and structural parameters for CH_4 adsorbed on top of the Ni adatom with several possible orientations

Adsorption sites	Adsorption energy (eV)	Longest C–H bond length (Å)	C–Ni distance (Å)	Largest H–C–H angle (°)	Smallest H–C–H angle (°)
t1	0.14	1.116	3.116	110.4	108.5
t2	0.37	1.129	2.185	115.3	107.5
t3	0.25	1.112	2.200	111.4	107.0

energetic data in Table 2 shows unambiguously that in presence of the adatom, the nature of the interaction of Ni with the molecule has evolved toward a weak chemical bond, with an adsorption energy change t2 > t3 > t1. As previously, the t2 configuration is the best with 0.37 eV to be compared with 0.05 eV on the flat surface. The C–Ni distances are all shorter than in Table 1, the shortest corresponding to t2 with 2.185 Å. We note that the C–Ni distance is only 0.015 Å longer for t3 in spite of a clear energetic loss by 0.12 eV. The structural consequences for the molecule are clearly visible. The C–H bond length increases when the H atom is directed to the surface, up to 1.129 Å for t2. The angular distance between the C–H bonds is also affected, the biggest difference between the largest and smallest angle being recorded for t2. This angle is contracted with respect to the free molecular value when it involves 1 H pointing to the surface and a second one pointing to the vacuum, revealing some attraction between the two bonds. On the contrary, it opens when both H atoms point toward the surface or the vacuum.

The PDOS of the adsorbed molecule with t2 configuration is reported on Fig. 6. We note that, due to the low work-function of the covered surface (4.96 eV), some unoccupied C s states of the free molecule are now visible below +5 eV whereas they were beyond this limit in Fig. 4. Actually, the clean surface work-function was already low (5.62 eV) with respect to the perfect Ni(1 1 1) surface (5.92 eV). Hence the work-function lowering originating from to the molecular adsorption is $\Delta\Phi = 0.66$ eV showing that the polarisation between the surface and the molecule is now bigger than on the perfect surface. As a consequence, the α peak (−14.70 eV) is now shifted by 2.75 eV to high binding energies with respect to the gas phase. The β peak is now split in two components located at −7.40 eV (β') and −6.90 eV (β''), hence shifted by 3.0 eV and 2.5 eV, respectively from the gas phase. The electronic states contributing to β' are mainly C p*z* and H s states. We outline that only the H atoms directed to the surface are involved in β'. β'' is mainly derived from

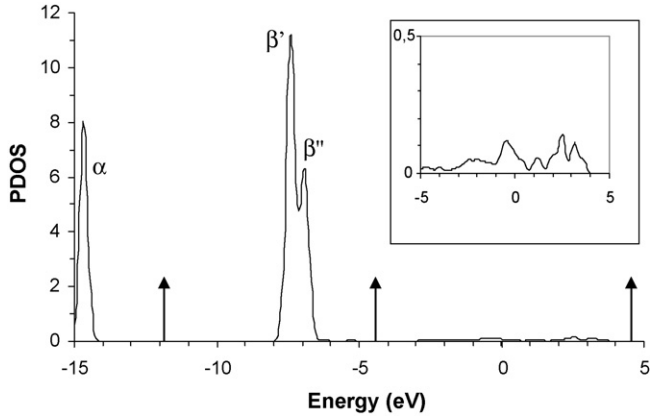

Fig. 6. Projected density of states of the CH_4 molecule adsorbed in the t2 configuration on the defective Ni(1 1 1). A zoom on the Fermi level region in given as inset. The position of the free molecule levels with respect to the covered Ni vacuum level is indicated by vertical arrows. The Fermi level is the origin of the energy scale.

C p*x* and p*y* states and s states from the H directed toward the vacuum. As α is the farthest from the Ni band region, we can take its shift as essentially the result of the molecule/surface polarisation. Hence, the supplementary shift (0.25 eV) suffered by β' would be the result of a stabilising interaction due to the surface whereas the negatively shifted β'' (−0.25 eV) indicates a repulsion from the surface. This also means that the C sp^3 hybridisation is partially lifted. For the H atoms directed to the vacuum, this results in a preferential interaction with C p*x* and p*y* states. A direct consequence is that these H atoms are pushed toward the *xy* plane going through C to improve the s(H)-p*x*(C) and s(H)-p*y*(C) overlap. An unexpected result is the narrowing of the angular distance between the H pointing toward and backward the Ni surface.

Fig. 6 inset shows the −5 eV +5 eV region where weak states resulting from a mixture with the Ni states are apparent. The main features are around −0.5 eV, 1 eV, 2.5 eV and 3 eV. They are essentially C p*x* and p*y* and H s states in the occupied region. The main contributing unoccupied states are C sp states. In all the region from −5 eV up to 5 eV, the localised features are superimposed on a more or less continuous C p*z* background. The overall occupation shows that CH_4 loses 0.13 electron. Charge is lost from H s states, again mainly from the H atoms directed to the surface, and C p*z* states. This shows that the O(CH_4)–U(Ni) interaction is largely more efficient than it was on the perfect Ni(1 1 1) surface. We note that for CH_4 adsorbed with the t3 configuration, the total charge loss is again 0.13 electron, but this loss is essentially from H states without clear distinction between the H atoms of the molecule. There is no sizeable loss from C states for t3. Finally, for t1 configuration, there is only a minute charge lost by CH_4. It is essentially the result of a loss from C p*z* states and a C p*x* and p*y* gain, whereas the H s loss is largely reduced. From the comparison between the various configurations, we note that the stability of the adsorbed molecule and its structural modifications are qualitatively in line with the H s loss following the order t2 > t3 > t1. The Ni adatom occupation count does not reveal a sizeable change upon CH_4 adsorption but shows an electron redistribution: a dz^2 loss is counterbalanced by a gain, mainly from d*xz* and d*yz* states. Again the degree of occupation change follows the order t2 > t3 > t1.

The Ni sp PDOS changes induced by CH_4 on the Ni adatom show, as in the previous paragraph, that this interaction is of secondary importance. Examination reveals essentially s and p*z* gain in resonance with the α and β features detected on the molecule. States of similar symmetries are lost from −6 eV up to −3 eV, and more importantly above the Fermi level. This suggest that s-p*z* filling make this interaction essentially non-bonding. We report on Fig. 7 the dz^2 and d*xz* change suffered by the adatom, calculated as a difference between the respective PDOS after and before CH_4 adsorption. The evolution of the other Ni valence states are not reproduced. Both curves exhibit a resonance feature with the molecular states around −7.5 eV. States are lost at the Fermi level for *dxz* and around −0.4 eV on the dz^2 curve. Note that the loss on dz^2 is about 3 times that on d*xz*. New dz^2 occupied states are noted around −1 eV and −2 eV and unoccupied states from 0 eV up to 3 eV, showing that this is a channel for Ni to molecule back-

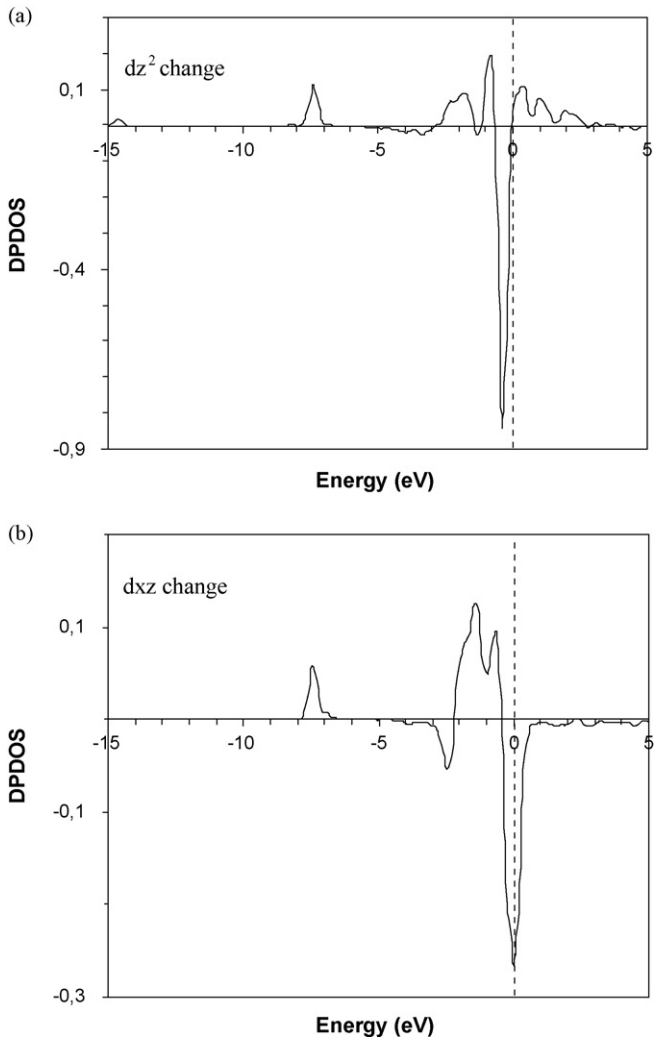

Fig. 7. Ni d projected density of states change upon CH_4 adsorption on the Ni adatom plotted for dz^2 (a) and d*xz* (b). The Fermi level is the origin of the energy scale.

donation. Occupied d*xz* states are gained around −1 eV and −1.5 eV, but unoccupied states are lost around FL showing that this band is pushed down hence receiving some electron charge from the molecule. This picture suggests a bonding interaction of the adatom with the molecule involving essentially dz^2 states on one side, C sp states on the other side, with possibly some participation of H s states.

We outlined previously the narrow 3d-band of the Ni adatom with respect to the flat surface (Fig. 1). Moreover, its valence d-band exhibit a high density around −0.4 eV which is not present on the Ni(1 1 1) surface. We note that it is 28 % of dz^2 nature, in good correlation with the above mentioned dz^2 loss upon CH_4 adsorption. The position of the d-band centre as a parameter monitoring the surface reactivity has already been stressed concerning CO adsorption [35] and generalised to various molecule-surface systems [36,37]. The argument is that the higher the d-band centre, the stronger is the interaction between the metal surface d states and the frontier orbitals of the molecule. Here the d-band centre is located at −1.45 eV on the Ni(1 1 1) surface and −0.99 eV on the adatom. Indeed the interaction of the d-band with the molecular states are apparent upon CH_4 adsorption on the adatom. The dz^2 states split, some being stabilised as a result of the interaction with C p states, some of them being pushed up to the unoccupied region. This gives rise to a loss of dz^2 count but result in a net attraction of the molecule to the surface. On the molecular side of the adsorbed system, adsorption induces a H s electron loss, depleting the H–C sp bond which become less attractive. All these features are visible for CH_4 adsorbed on the adatom and to a far lesser degree on the perfect surface, meaning that the same basic chemical mechanism is at play in both case. However in the former case, the stronger interaction of the molecular states with the adatom d-band makes the chemical character of the interaction to be fully recognisable. Such a chemical interaction between a metal surface and a hydrocarbon molecule is in good qualitative agreement with the experimental findings of Ötröm et al. [34] concerning the octane/Cu(1 1 0) system. Another model was also proposed to analyse this interaction [38]. It involves a small back-donation from Cu to the molecule, whereas the donation from the latter to the metal is negligible. On the contrary, our results show a noticeable net electron loss from the molecule.

Finally, it is of interest for the full picture understanding to invoke a recent paper by Philipsen and Baerends [39]. The interaction of a molecule with a surface was studied with help of energy decomposition analysis. For N_2 on W(1 0 0), they show that the occupied-occupied orbitals repulsive (Pauli) interaction starts rising for molecule-surface distances around 4 Å but is slightly overbalanced by occupied-unoccupied (chemical) and electrostatic interaction giving a small net bonding (by 0.03 eV) between the molecule and the surface. Their results go largely beyond the specific examples illustrated by the authors. Indeed, this attraction range and the N_2-surface distance are similar to those reported in the present work for CH_4/Ni(1 1 1). Moreover, it is shown in ref. [39] that at shorter distances, the Pauli repulsive interaction become dominant until it can be relieved when the antibonding part of the occupied-occupied interaction rises above the metal Fermi level (E_f). For N_2/W, this happens below 3 Å so that the full chemical stabilisation is obtained around 2 Å. On the contrary, for CH_4/Ni most of these antibonding states are still below Ef even in presence of an adatom, limiting the net attractive energy at a low level. Finally, for a strong enough coupling, the bonding levels resulting from unoccupied–unoccupied interaction drop below E_f, giving a supplementary bonding and relief of the Pauli repulsion. Here, we can find these states in the 2–4 eV region above the Fermi level on Fig. 5 showing that they play no role for CH_4 interaction with the Ni perfect surface. However, they are probably pushed down close to E_f in presence of the adatom (Fig. 7a). The lost just above and below E_f on Fig. 7 as well as occupied states gained at −1 eV and below could suggest that they start to be occupied whereas some antibonding states from the occupied-occupied interaction are pushed up above E_f.

4. Conclusions

A DFT plane wave approach was used with a slab model to investigate the methane molecular adsorption on Ni(1 1 1). We have found that the interaction of the molecule with the perfect surface is very weak and largely of physical origin. However, some features revealing a weak chemical interaction could be put in evidence. This chemical interaction become sizeable when CH_4 is adsorbed on top of a Ni adatom. It involves Ni d electrons, mainly dz^2, d*xz* and d*yz*, together with distribution change, a dz^2 loss being more or less counterbalanced by d*xz* and d*yz* gain. H–C bonds weakening is induced, due to sp electron loss from the molecule. The Ni adatom enhanced reactivity is a consequence of the valence-band centre up-shift resulting from the Ni coordination reduction. Similar features can be recognised to a far lesser extend when the molecule is adsorbed on the flat surface. In both case, the orientation of the molecule with 2 H atoms directed to the surface is the most favourable. We suggest that, when the chemical interaction dominates, this can be the result of a compromise as

this configuration favours a direct attractive interaction between the Ni adatom and the C atom of the molecule (over the t1 configuration) whereas a repulsive interaction with the hydrogen atoms would be too high in the t3 configuration. Finally, these results suggest that in presence of Ni adatoms the dissociative pathway of CH_4 from an adsorbed precursor could be of interest.

Acknowledgement

Support from the ''Réseau Alsace de Laboratoires en Ingénierie et Sciences pour l'Environnement'' REALISE is acknowledged.

References

[1] F. Zaera, Chem. Rev. 95 (1995) 2651.
[2] V.T. Choudhary, E. Akosoylu, D.W. Goodman, Catal. Rev. 45 (2003) 151.
[3] C.N. Stewart, G. Ehrlich, J. Chem. Phys. 62 (1975) 4672.
[4] J.F. Weaver, F.A. Carlson, J.R. Madix, Surf. Sci. Rep. 50 (2003) 107.
[5] A.T. Gee, B.E. Hayden, C. Mormiche, J. Chem. Phys. 118 (2003) 3334.
[6] A.C. Luntz, J. Chem. Phys. 102 (1995) 8264.
[7] M.N. Carré, B. Jackson, J. Chem. Phys. 108 (1998) 3722.
[8] Y. Xiang, J.Z.N. Zhang, J. Chem. Phys. 118 (2003) 8954.
[9] P. Kratzer, B. Hammer, J.K. Nørskov, J. Chem. Phys. 105 (1996) 5595.
[10] A.T. Anghel, D.J. Wales, S.J. Jenkins, D.A. King, Phys. Rev. B 71 (2005) 113410.
[11] A.C. Luntz, H.F. Winners, J. Chem. Phys. 101 (1994) 10980.
[12] W.H. Wienberg, J. Vac. Sci. Technol. A 10 (1992) 2271.
[13] P.M. Holmblad, J. Wambach, I. Chorkendorff, J. Chem. Phys. 102 (1995) 8255.
[14] C.R. Arumainayagam, M.C. McMaster, G.R. Schoofs, R.J. Madix, Surf. Sci. 222 (1989) 213.
[15] A.C. Luntz, D.S. Bethume, J. Chem. Phys. 90 (1989) 1274.
[16] A.V. Hamza, R.J. Madix, Surf. Sci. 179 (1987) 25.
[17] M.B. Lee, Q.Y. Yang, S.T. Ceyer, J. Chem. Phys. 87 (1987) 2724.
[18] T.M. Beebe Jr., D.W. Goodman, B.D. Kay, J.T. Yates Jr., J. Chem. Phys. 87 (1987) 2305.
[19] A.G. Sault, D.W. Goodman, J. Chem. Phys. 88 (1988) 7232.
[20] K.M. DeWitt, L. Valadez, H.L. Abbott, K.W. Kolasinski, I. Harrison, J. Phys. Chem. B 110 (2006) 6705.
[21] G. Henkelman, H. Jonsson, Phys. Rev. Lett. 86 (2001) 664.
[22] G. Fratesi, S. de Gironcoli, J. Chem. Phys. 125 (2006), 044701.
[23] Ab initio pseudopotential code Dacapo (version 2.7.3, 2003), developed at CAMPOS (Center for Atomic-Scale Materials Physics, Department of Physics, Technical University of Denmark, Lyngby; see http://www.fysik.dtu.dk for details).
[24] D. Vanderbilt, Phys. Rev. B 41 (1990) R7892.
[25] J.P. Perdew, J.A. Chevary, S.H. Vosko, K.A. Jackson, M.R. Pederson, D.J. Singh, C. Fiolhais, Phys. Rev. B 46 (1992) 6671.
[26] D.R. Lide (Ed.), CRC Handbook of Chemistry and Physics, 76th ed., CRC Press, New York, 1996.
[27] J. Greeley, M. Mavrikakis, Surf. Sci. 540 (2003) 215.
[28] C.-T. Au, C.-F. Ng, M.-S. Liao, J. Catal. 185 (1999) 12.
[29] H. Yang, J.L. Whitten, J. Chem. Phys. 96 (1992) 5529.
[30] W. Lai, D. Xie, D.H. Zhang, Surf. Sci. 594 (2005) 83.
[31] P.S. Moussounda, M.F. Haroun, B. M'Passi-Mabiala, P. Légaré, Surf. Sci. 594 (2005) 231.
[32] D.C. Sorescu, Phys. Rev. B 73 (2006), 155420.
[33] Y. Morikawa, H. Ishii, K. Seki, Phys. Rev. B 69 (2004), 041403 (R).
[34] H. Öström, L. Triguero, M. Nyberg, H. Ogasawara, L.G.M. Pettersson, A. Nilsson, Phys. Rev. Lett. 91 (2003), 046102.
[35] B. Hammer, Y. Morikawa, J.K. Norskov, Phys. Rev. Lett. 76 (1996) 2141.
[36] K. Abild-Pedersen, O. Lytken, J. Engæk, G. Nielsen, I. Chorkendorff, J.K. Norskov, Surf. Sci. 590 (2005) 127.
[37] B. Hammer, Topics Catal. 37 (2006) 3.
[38] Ch. Wöll, K. Weiss, P.S. Bagus, Chem. Phys. Lett. 332 (2000) 553.
[39] P.H.T. Philipsen, E.J. Baerends, J. Phys. Chem. 110 (2006) 12470.